MSFC-057

APPLICATION OF SEMI ACTIVE CONTROL TECHNIQUES TO THE DAMPING SUPPRESSION PROBLEM OF SOLAR SAIL BOOMS.

O. Adetona and L.H. Keel
Tennessee State University
Nashville, Tennessee

M.S. Whorton
NASA Marshall Space Flight Center
Huntsville, Alabama

ABSTRACT

Solar sails provide a propellant free form for space propulsion. These are large flat surfaces that generate thrust when they are impacted by light. When attached to a space vehicle, the thrust generated can propel the space vehicle to great distances at significant speeds. For optimal performance the sail must be kept from excessive vibration. Active control techniques can provide the best performance. However, they require an external power-source that may create significant parasitic mass to the solar sail. However, solar sails require low mass for optimal performance. Secondly, active control techniques typically require a good system model to ensure stability and performance. However, the accuracy of solar sail models validated on earth for a space environment is questionable. An alternative approach is passive vibration techniques. These do not require an external power supply, and do not destabilize the system. A third alternative is referred to as semi-active control. This approach tries to get the best of both active and passive control, while avoiding their pitfalls. In semi-active control, an active control law is designed for the system, and passive control techniques are used to implement it. As a result, no external power supply is needed so the system is not destabilize-able. Though it typically under-performs active control techniques, it has been shown to out-perform passive control approaches and can be unobtrusively installed on a solar sail boom. Motivated by this, the objective of this research is to study the suitability of a Piezoelectric (PZT) patch actuator/sensor based semi-active control system for the vibration suppression problem of solar sail booms. Accordingly, we develop a suitable mathematical and computer model for such studies and demonstrate the capabilities of the proposed approach with computer simulations.

INTRODUCTION

Solar sails can propel a space vehicle using thrust generated when energy of photons from the sun are reflected from large flat surfaces. Though the force generated is small, propellants are not required and the space-craft can achieve large velocities because the external force acts for the life of the mission ([1],[2]). A Solar Sail configuration to address NASA's future propulsion needs is under development by a team from L'Guarde, Jet Propulsion Laboratories, Ball Aerospace, and NASA Langley Research Center ([1], [2]). This 100m square sail configuration consists of four identical quadrants each containing a triangular sail. The four sails (made from Mylar) are supported by four booms (at right-angles to each other) attached to the solar sail craft. Control vanes (small reflective areas) that resemble a scaled quadrant are attached to the free tip of each boom via actuators. Thrust is vectored by rotating the vanes around the boom axis. Full three axis control is achieved by actuating three (or four) vanes simultaneously [2].

The efficiency with which energy from the reflected photons is converted into solar sail thrust will be affected by sail flatness. Since solar sails have no inherent bending stiffness, and little mass, sail dynamics will be dominated by boom dynamics. In addition, the booms are long, flexible, and

lightly damped structures. Therefore, disturbances to the boom (typically a truss) can result in large amplitude, long duration vibration motion that will have a debilitating impact on the performance [3]. Minimizing the adverse effects of this vibration will require vibration mitigation technologies. Piezo-electric (PZT) actuation devices can convert mechanical vibration energy to electrical energy and vice versa. They also have wide frequency response spectrum and strong electro-mechanical coupling. If bonded to the surface of a flexible structure, they are conceptually capable of operation in the space environment and can therefore be classified as "space-realizable" [3]. Furthermore, thin, light-weight and flexible PZT actuators such as polyvinyledine (PVDF) film and a macro-fiber composite patch can be packaged in an inobtrusive manner on (or within) the truss such as the L'guard Truss without introducing significant mass loading. For these reasons, PZT devices have been extensively used as sensors and actuators for active and passive vibration suppression of flexible structures [4].

Active control of vibration involves utilization of powered actuation devices and easily benefits from modern control design techniques. Consequently it can potentially provide the best performance for a given hardware configuration. However, it requires a significant external energy source to drive the actuators and can destabilize the structure if improperly designed [5]. Furthermore the required energy source will introduce significant parasitic masses, and thus this approach is not well suited to solar sail craft where low masses are critical. Passive approaches have the advantage that they can not destabilize the system under any circumstances because they only take vibration energy out of the structure. In this approach a Piezo-electric actuator is shunted (e.g. with a resistor or resistor and actuator). As a result, mechanical vibration energy is converted to electrical energy, which is then dissipated via a passive circuit. This approach typically under-performs active approaches and may require large inductance (i.e. a heavy coil) for low frequency vibration suppression. Since the boom is long and light weight, the dominant modes will have a low frequency. Therefore a heavy coil may be required for each actuator. Since several actuators may be needed, the large total mass of all the coils makes passive control with PZT devices un-ideal for ultra-light weight structures like solar sail craft.

Recently a new vibration suppression approach called "semi-active" or "hybrid" vibration suppression has been introduced. The idea is to convert vibration energy to electrical energy via PZT actuators attached to the vibrating structure, accumulate the electrical energy, and then dissipate the stored energy in a controlled manner. For example, a resistive, capacitive or inductive shunt circuit (for the PZT actuator) is switched on and off according to the phase of a vibrating mode of the structure [5]. Since vibration energy is always extracted from the system, this approach cannot destabilize the system. A benefit of this approach is the fact that external power to drive the actuators is not needed. However, a small external energy source may be needed to power the switching circuit. In view of the above, semi-active control techniques are well suited to vibration suppression of a solar sail boom. However, research on this approach is limited and further studies are needed.

In Reference 6, we showed that a solar sail boom could be modeled as an Euler-Bernoulli beam with clamped-free boundary conditions. As an extension of this effort, we herein use an Euler-Bernoulli beam to illustrate the capabilities of semi-active vibration suppression for solar sail booms. We begin by developing a mathematical model of a classical Euler-Bernoulli beam with clamped-free boundary conditions and integrated PZT actuators/sensors. The model can accommodate multiple PZT actuator/sensor patches at arbitrary locations on the beam. Next we validate the model with experimental input-output data. Since models of solar sail booms are expected to contain significant uncertainties, we consider an active control law (in this case velocity feedback) that is inherently robust to model uncertainties. Semi-active control is then simulated as a switching logic that causes the charge generated in the PZT actuators (due to beam vibration) to have the same sign as the charge that would be induced in the actuator by the active control law in a single degree of freedom system. The results of the simulation are provided and compared with equivalent results if a passive approach had been used.

EXPERIMENTAL SETUP

The test setup is shown in Figure 1. A galvanized steel beam was clamped at one end and free to move at the other end. A pair of Macro Fiber Composite (MFC) PZT patches (manufactured by smart material corporation) were glued to opposite sides of the beam close to the clamped end and wired so that their individual response to an identical voltage will be 180^0 out of phase. A laser displacement sensor was used to measure the beam displacement at the farthest point on the patch from the clamp (i.e. 56mm from the clamp). Additional details are provided below.

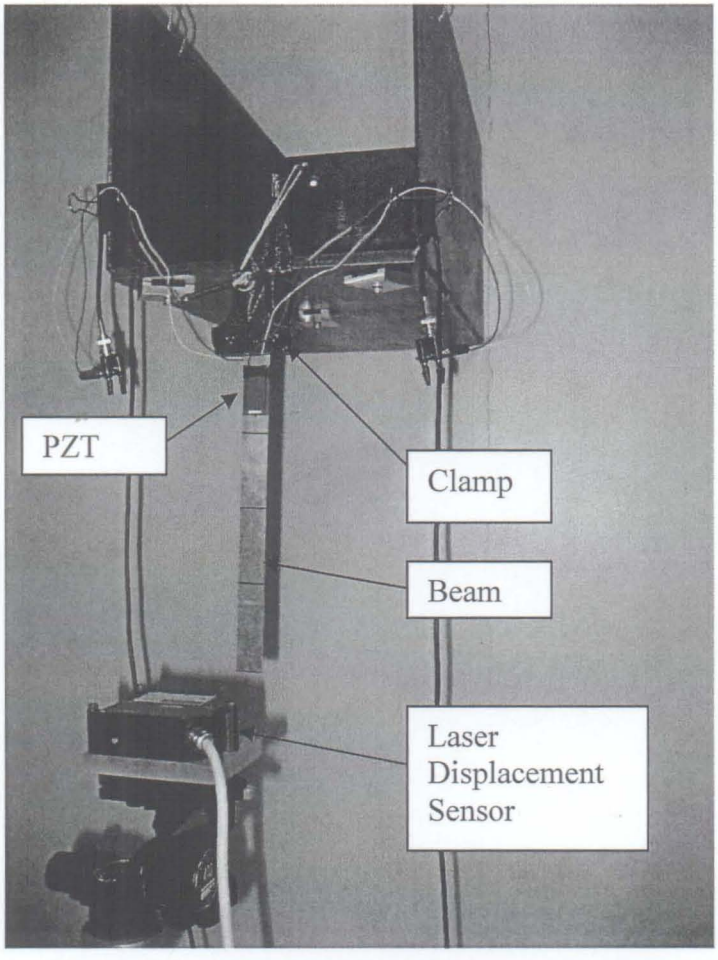

Figure 1: Test Setup

PROPERTY	SYMBOL	VALUE
Modulus of Elasticity of the (Steel) Beam	E_B	207×10^9 N/M^2
Modulus of Elasticity of the PZT	E_p	30.336×10^9 N/M^2
Density of the (Steel) Beam	ρ_B	7850 Kg/M^3
Free Strain per volt (average of: Low field ~ High field)	d_{33}	0.75 ~ 0.9 ppm/Volt
Apparent Internal Capacitance of the PZT Actuator	Ca	1.7052×10^{-9} F
PZT Actuator Input Voltage Range		-500V ~ +1500V

Table 1: Material Properties

PARAMETER	SYMBOL	VALUE
Length of the beam (from clamped point to free end)	L_B	288mm
Beam Width	W_B	25.4mm
Beam Thickness	t_B	0.508mm
Location of each MFC patch from clamped end		16mm ~ 56mm
Length of each MFC patch		40mm
Width of each MFC patch		25.4mm
Length of active area (Epoxy + PZT at center) of MFC patch	L_P	
Width of active area (Epoxy + PZT at center) of MFC patch	W_P	14mm
Thickness of active area (Epoxy + PZT at center) of MFC patch	t_P	29mm
Thickness of epoxy alone (around the edges) of MSFC patch		14mm

Table 2: Dimensions

TEST PROCEDURE

To obtain validation data for the physics model, a 1 Hz square wave with amplitude 1 Volt was generated with a National Instruments data acquisition system and then amplified (with a Trek Model PZD 700-2-L-CE Piezo Driver/Amplifier) by a factor of 200. A laser displacement sensor (ILD 1800-200 made by Micro Epsilon) was used to measure the displacement of the Beam/PZT at 56mm from the clamp point at a sample rate of 1000Hz. The Frequency response functions of the input-output data were computed with the MATLAB spafdr function, while sixth order models were identified with the n4sid in the MATLAB System Identification toolbox. The validated model was subsequently used for the simulations presented herein. In this study the vibration suppression schemes will be designed to target the first vibration mode. Accordingly, an "optimal" inductance L for passive vibration suppression is $L = 1/\omega^2 C_a$ where ω is the natural frequency of the first mode in radians per second, and C_a is the inherent capacitance of the PZT actuator. Similarly, an optimal value of inductance for semi-active control is $L = 0.1/\omega^2 C_a$.

MATHEMATICAL MODEL

Assumptions:

1. Beam has a uniform mass distribution and a uniform stiffness, that are $m(s) = m$ and $EI(s) = EI$ respectively.

2. Perfectly straight beam.

3. External forces and moments do not induce any torsional effects.

4. Cross-sectional dimensions are small compared to beam length. Note that shear and rotary inertia effects can be neglected under this assumption. However, these effects become significant as mode number increases.

5. Small bending deformations, specifically: $\left(\frac{dy}{ds}\right)^2 << 1$.

6. The beam is stiff in the axial direction, so length change due to axial forces is negligible.

EQUATION OF BENDING MOTION

We considered a beam clamped at one end and free at the other end and derived equations of transverse motion $y(s,t)$ in response to applied forces and moments. At rest, the beam is vertical to minimize gravity effects and thereby simulate the zero gravity effects of space. Its system equation for bending motion is ([6] and [7]):

$$\frac{\partial^2}{\partial s^2}\left[EI\frac{\partial^2 y}{\partial s^2}\right] - T(L)\frac{\partial^2 y}{\partial s^2} + mg\left((s-L)\frac{\partial^2 y}{\partial s^2} + \frac{\partial y}{\partial s}\right) + m\frac{\partial^2 y}{\partial t^2} = w(s,t) - \frac{\partial^2 M(s,t)}{\partial s^2} \qquad (1)$$

where s is the longitudinal spatial coordinate, y is the transverse displacement, EI is the bending stiffness, $T(L)$ is axial tension at $s = L$, m is the mass per unit length, L is the length of the beam, t is time, w is the spatially distributed transverse force and M is the applied moment per unit length.

We used *admissible* functions in our analysis because of difficulties computing the mode shape functions $\phi_j(s)$. The *admissible* functions are the mode shape functions

of the classical Euler-Bernoulli Beam, i.e:

$$u_j(s) = c_{1j}\sin(\beta_j s) + c_{2j}\cos(\beta_j s) + c_{3j}\sinh(\beta_j s) + c_{4j}\cosh(\beta_j s) \qquad (2)$$

where β_j, and c_{1j}, c_{2j}, c_{3j}, c_{4j}, $j = 1,2,3,...$ are computed from boundary conditions.

BENDING MOMENTS DUE TO PZT PATCHES

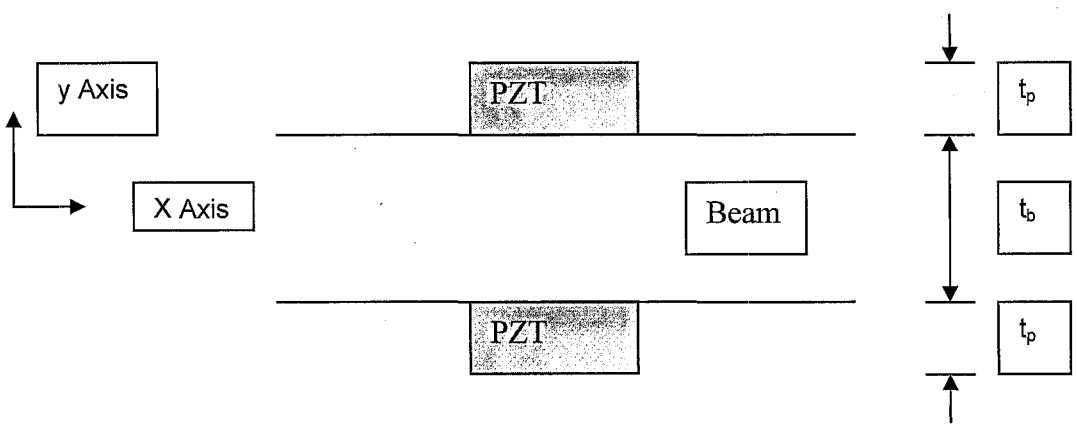

Figure 2: Cross-sectional view of PZT Actuator Pair on a Beam

The active area of the PZT patches on our test-bed is not as wide as the beam even though the PZT patch and the beam have the same width. Though many texts (e.g. [8]) provide physics equations for a beam with integrated PZT actuators, we are not aware of any results that explicitly accounts for the case where PZT patches have a different width from the beam. Motivated by

this, we developed physics models for the case where several such PZT patches are attached to arbitrary locations along an Euler-Bernoulli beam. Our models consider the case where the PZT patches are used as actuators or sensors. Such models capture the dual actuator/sensor nature of PZTs needed for our study.

Figure 2 shows a cross-sectional view of a beam with thickness t_b that has two PZT patches (each with thickness t_p) at opposite sides of the beams longitudinal axis. The strain ε_p in the PZT is:

$$\varepsilon_p = \frac{d_{33} V_A}{L_p}.$$

where V_A is the voltage applied to the MFC PZT patch across its 3 direction. We assume a linear strain distribution $\varepsilon(z)$ across the Beam/PZT cross-section induced by the PZT patch pair is given by

$$\varepsilon(z) = \alpha\ z.$$

Note that stress is not continuous though strain is. From Hookes' law:

$$\sigma_b(z) = E_b \varepsilon(z) = E_b\ \alpha\ z$$

where E_b is the Elastic modulus of the beam. For the case where the voltage applied to the top PZT is 180° out of phase with that applied to the bottom PZT, we get:

$$\text{Top PZT:} \quad \sigma_p^T = E_p \alpha\ z - E_p \varepsilon_p = E_p(\alpha\ z - \varepsilon_p)$$
$$\text{Bottom PZT:} \quad \sigma_p^B = E_p \alpha\ z + E_p \varepsilon_p = E_p(\alpha\ z + \varepsilon_p)$$

where E_p is the Elastic modulus of the PZT. For equilibrium about the center of the beam, we have

$$0 = \underbrace{w_p \int_{-\frac{t_b}{2}-t_p}^{-\frac{t_b}{2}} \sigma_p^B(z) z dz}_{Moment\sim due\sim to\sim bottom\sim PZT} + \underbrace{w_b \int_{-\frac{t_b}{2}}^{\frac{t_b}{2}} \sigma_b(z) z dz}_{Moment\sim on\sim beam} + \underbrace{w_p \int_{+\frac{t_b}{2}}^{\frac{t_b}{2}+t_p} \sigma_p^T(z) z dz}_{Moment\sim due\sim to\sim top\sim PZT}.$$

We can solve for α by integrating the expression above to get

$$\alpha = \frac{3E_p w_p \left(\left(\frac{t_b}{2} + t_p \right)^2 - \left(\frac{t_b}{2} \right)^2 \right)}{2\left(E_p w_p \left\{ \left(\frac{t_b}{2} + t_p \right)^3 - \left(\frac{t_b}{2} \right)^3 \right\} + E_b w_b \left(\frac{t_b}{2} \right)^3 \right)} \varepsilon_p .$$

Therefore the induced moment per unit length M_p in the beam due to the PZT patches is:

$$M_p(t) = E_b I_b \alpha(t) = E_b I_b \underbrace{\left[\frac{3E_p w_p \left(\left(\frac{t_b}{2} + t_p \right)^2 - \left(\frac{t_b}{2} \right)^2 \right)}{2\left(E_p w_p \left\{ \left(\frac{t_b}{2} + t_p \right)^3 - \left(\frac{t_b}{2} \right)^3 \right\} + E_b w_b \left(\frac{t_b}{2} \right)^3 \right)} \right] \frac{d_{33}}{L_p}}_{K_{V_A}} \cdot V_A(t) \qquad (3)$$

where $I_b = \frac{w_b t_b^3}{12}$ is the moment of inertia of the beam. Next we calculate $\int_0^L \phi_i(s) \frac{\partial^2 M_p(s,t)}{\partial s^2} ds$ which is needed to compute transverse forces induced in the beam by the PZT patches. Let $M_{pj}(s,t)$ denote the moment due to the j^{th} PZT patch (from a set of m_2 actuator pairs) located at $a_j \le x \le b_j$, and $V_{A_j}(t)$ is the voltage applied to the actuator, then

$$M_p(s,t) = \sum_{j=1}^{m_2} M_{pj}(s,t)$$

with

$$M_{pj}(s,t) = K_{V_A} V_{A_j}(t) \left(U(s-a_j) - U(s-b_j) \right)$$

where K_{V_A} is a constant implicitly defined in eq. (3) and $U(\cdot)$ is the unit step function. From the definition of Dirac's delta function, we have

$$U(s-z) = \int_{-\infty}^{0} \delta(x-z)dx .$$

Therefore

$$M_{pj}(s,t) = K_{V_A} V_{A_j}(t) \int_0^L \delta(x-a_j) - \delta(x-b_j)dx .$$

Accordingly for *i=1,2,…,n*:

$$\int_0^L \phi_i(s) \frac{\partial^2 M_p(s,t)}{\partial s^2} ds = \int_0^L \phi_i(s) \sum_{j=1}^{m_2} \frac{\partial^2 M_p(s,t)}{\partial s^2} ds = K_{V_A} \sum_{j=1}^{m_2} V_{Aj}(t) \left[\frac{\partial \phi_i(b_j)}{\partial s} - \frac{\partial \phi_i(a_j)}{\partial s} \right].$$

VOLTAGE GENERATED BY PZT PATCHES

From eq. (3), we have

$$M_p(t) = K_{VA} V_A(t) . \qquad (4)$$

It is well known that

$$M = \frac{EI}{r}$$

where r is the radius of curvature of a beam in flexure. Also we can set

$$\frac{1}{r} = \frac{d^2 y(x)}{dx^2}$$

assuming small deformations. Applying these two expressions to our system, we have

$$M_p(t) = E_b I_b \frac{d^2 y(x)}{dx^2}.$$

Equating the RHS of the expression above with the RHS of eq. (4) gives

$$E_b I_b \frac{d^2 y(x)}{dx^2} = K_{VA} V_A(t).$$

Assuming uniform flexural deformation due to the i^{th} PZT at $a_i \le x \le b_i$, we have

$$E_b I_b \frac{\partial^2 y(x)}{\partial x^2} = K_{VA} V_{Ai}(t).$$

For non-uniform flexure, we integrate the expression above from a_i to b_i and get

$$E_b I_b \int_{a_i}^{b_i} \frac{\partial^2 y(x,t)}{\partial x^2} dx = \int_{a_i}^{b_i} K_{VA} V_{Ai}(x,t) dx.$$

Next we assume the voltage-to-curvature equation above can be inverted as follows:

$$V_{G_i}(t) := \frac{E_b I_b}{K_{VA}(b_i - a_i)} \int_{a_i}^{b_i} \frac{\partial^2 y(x,t)}{\partial x^2} dx$$

Where $V_{G_i}(t)$ is the voltage generated in the I^{th} PZT (located at $a_i \le x \le b_i$) by flexure $\frac{\partial^2 y(x,t)}{\partial x^2}$ acting within $a_i \le x \le b_i$. Assuming separation of variables:

$$y(x,t) = \sum_{1}^{n} \phi_j(x) q_j(t)$$

we have

$$V_{G_i}(t) = \frac{E_b I_b}{K_{VA}(b_i - a_i)} \int_{a_i}^{b_i} \sum_{j=1}^{n} \frac{\partial^2 \phi_j(x)}{\partial x^2} q_j(t) dx = \frac{E_b I_b}{K_{VA}(b_i - a_i)} \sum_{j=1}^{n} \int_{a_i}^{b_i} \frac{\partial^2 \phi_j(x)}{\partial x^2} q_j(t) dx$$

Note that the preceding expression can be used for an arbitrary number of PZT patch pairs each of which can have arbitrary locations, width and thickness.

SIMULINK MODELS

We consider the case where the beam is initially excited by a 100 Volt external signal that acts on the transducer from time t=0.01 to t=0.011 seconds. Once excited, the resulting vibration is suppressed using either a passive or semi-active approach. This scenario was simulated in Simulink using Powergui (a graphical user interface for the analysis of circuits and systems). In this environment, the beam was represented by a transfer function computed from the physics model. For ease of exposition, we considered the collocated actuator/sensor case for which

velocity feedback is an appropriate active control strategy. Onoda et al. [5] demonstrated that semi-active vibration suppression is achieved by periodically shunting the terminals of a PZT transducer actuator across a series circuit consisting of an inductor and resistor according to the following simple rule. First design an active control signal (e.g. velocity feedback) and use it to compute the desired control signal U_Q. Next periodically discharge the charge Q built up in the PZT (due to vibration) such that $Q\,U_Q > 0$ whenever $U_Q > 0$. Accordingly, the following switching rule was devised to achieve this:

Turn on the switch when $U_Q\,V < 0$ and turn it off when $U_Q\,V > 0$,

where V is the voltage across the Transducer terminals. This switching logic was implemented in the Simulink diagram in Figure 2. Passive control was subsequently simulated by eliminating the switch in the Simulink diagram of Figure 2.

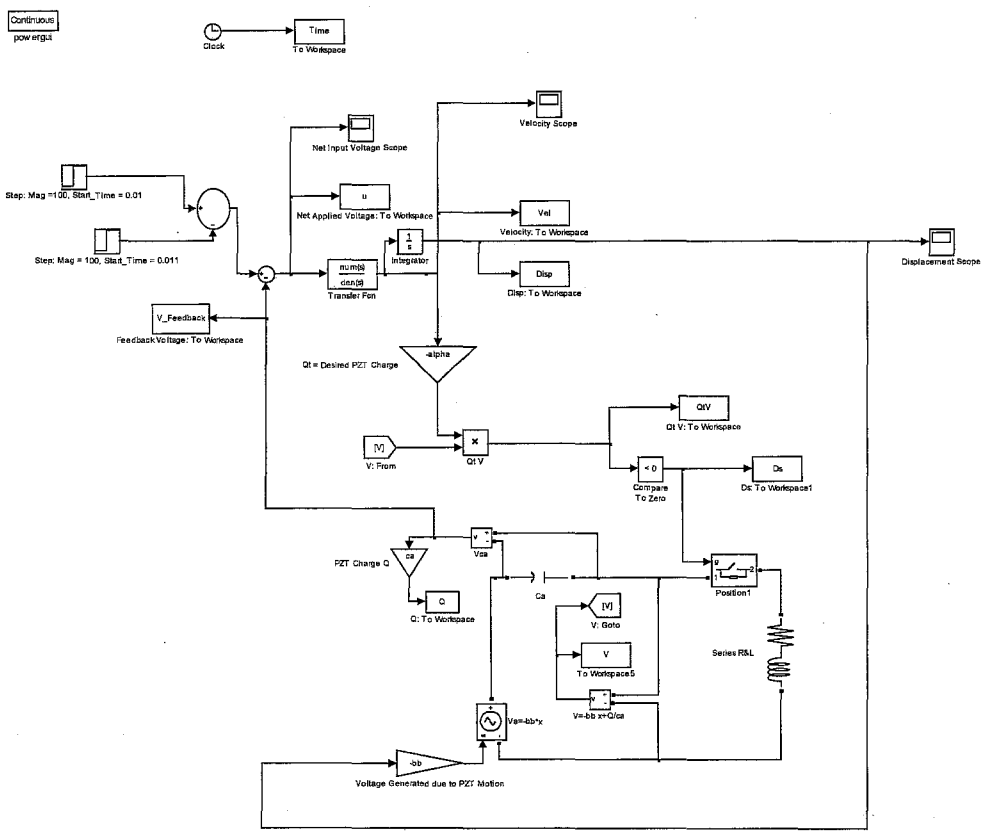

Figure 2: Simulink Model of the Beam under Semi-Active Control

RESULTS AND DISCUSSION

Onoda et. al [5] successfully implemented semi-active vibration control methods using PZT stack actuators. In their systems, the electrical energy generated when a PZT stack actuator is attached to a vibrating structure was dissipated passively in a manner that yields more vibration suppression than conventional passive methods. In our study, we plan to evaluate the effectiveness of their approach for structures with multiple integrated MFC PZT patches each of which has significantly lower inherent capacitance than conventional PZT stack actuators. As a first step, we developed a multi-actuator model and used it to study a beam with a co-located actuator pair.

MODEL VALIDATION RESULTS

First we consider the case where the PZT acts like a sensor. To study this, we used an impulse hammer to strike the beam at its free end and measured its response. The applied input force, transverse displacement, and generated voltage from both PZT actuator/sensors are provided in Figure 3. The fact that an impulse struck the beam around 2.2 seconds is evident from the PZT voltages in the bottom two plots of Figure 3, but not apparent from the Hammer and Laser Displacement plots at the top of Figure 3. Unfortunately, the magnitude of the applied force was apparently below the resolution of the impulse hammer and could therefore not be measured because of the noise. Similarly, a significant amount of ambient noise was present in the Laser displacement sensor signal.

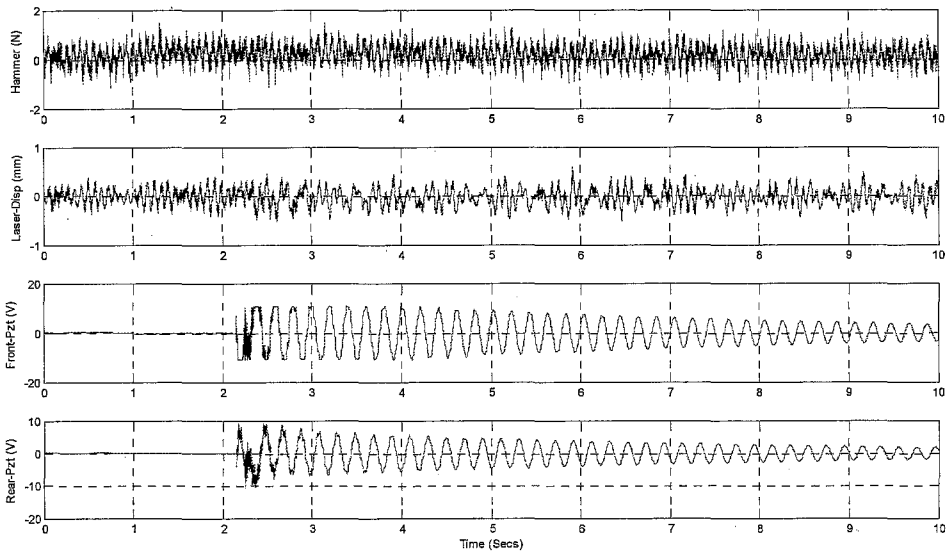

Figure 3: Input-Output Data for Impulse Force

The quality of the correlation between this set of input-output data was poor due to the presence of significant noise. This is evident from the incoherent appearance of the Frequency Response Function (FRF) computed from the raw data and the low magnitude and flat profile of the identified models. Consequently, the FRFs of Force-Input-to-Displacement-output of Figure 4, and the Force-input-to-Voltage-output of Figure 5 suffer from similar problems. However, the location of resonant peaks of the experimental data and the mathematical model appear to roughly match.

Next we obtained data for the case where the PZT acts as an actuator. Unfortunately, we had the same ambient noise problems again. The resulting FRF depicting the relationship between the applied voltage and beam displacement is depicted in Figure 6. In all cases the physics model had first second and third vibration mode natural frequencies of 5.0408, 32.3952, 89.8178 Hz respectively and a damping ratio of 0.01 was arbitrarily assumed for all three modes.

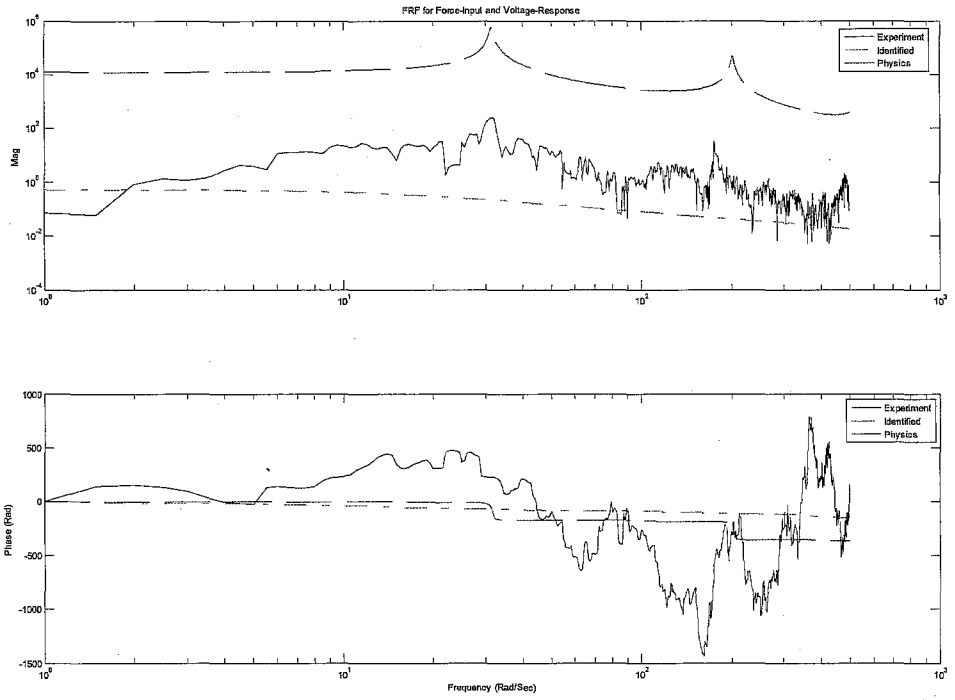

Figure 4: Frequency Response Plots for Force Input and Voltage Output

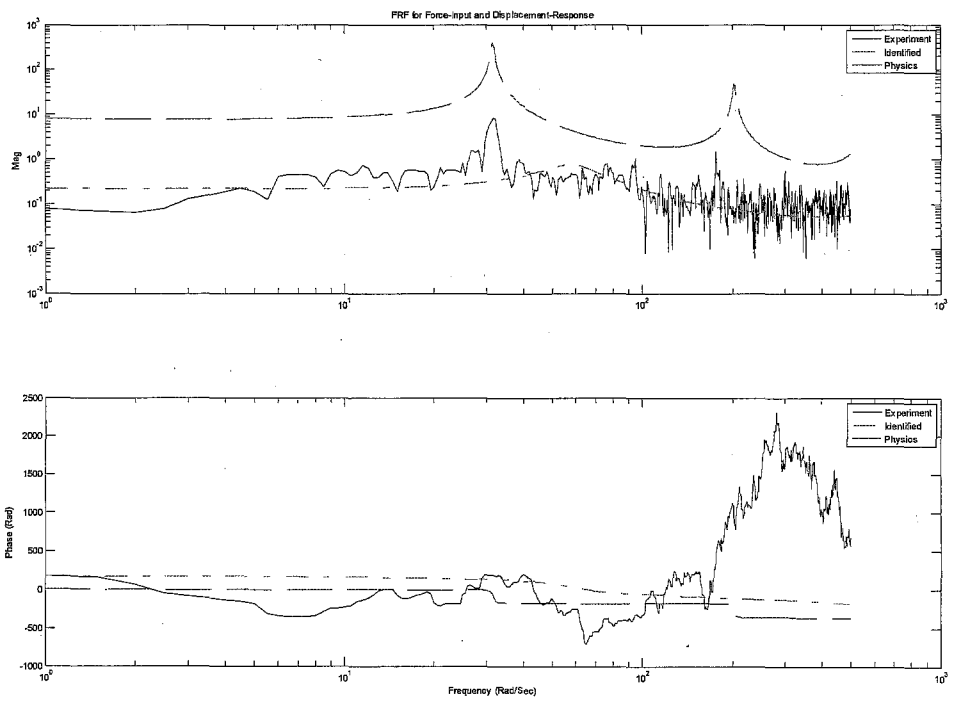

Figure 5: Frequency Response Plots for Force Input and Displacement Output

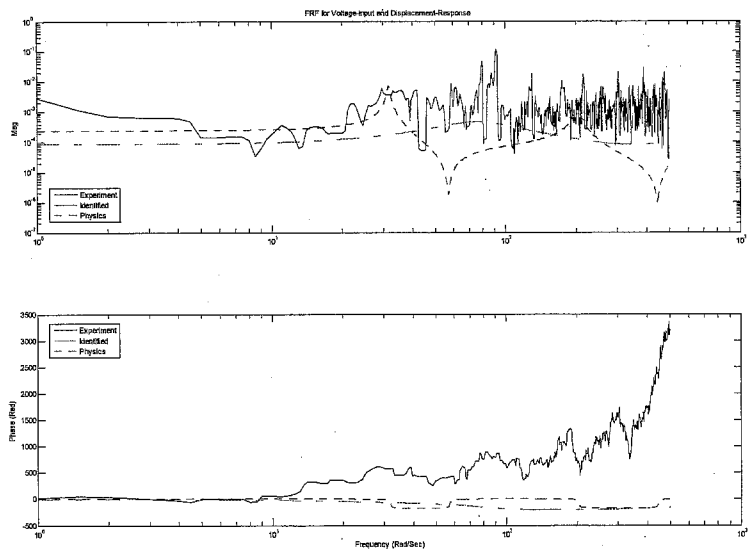

Figure 6: Frequency Response Plots for Voltage Input and Displacement Output

VIBRATION SUPPRESSION RESULTS

The results of the simulation of passive and semi-active vibration suppression are shown in Figure 7. The top part of Figure 7 shows the open loop (solid line) and closed loop (dashed line) response under passive control. Similarly, the bottom part of Figure 7 shows the open loop (solid line) and closed loop (dashed line) response under semi-active control. The superior performance of the semi-active control scheme is readily apparent.

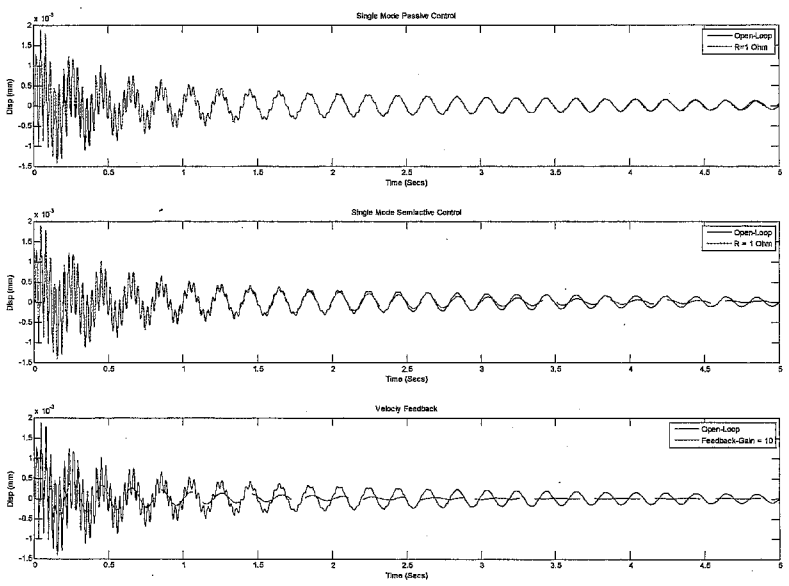

Figure 7, Responses: Passive (Top), Semi-Active (Middle) and Velocity Feedback (Bottom)

SUMMARY AND CONCLUSIONS

We demonstrated semi-active control with PZT actuators may be well suited to the vibration suppression problem of a long slender beam designed for solar sail craft. If a decentralized approach is used, there will be no need to run long cables and the system will be robust against failure of some of its sensors, actuators or controllers. Since only small external power is needed to power the control logic, the entire vibration control system should impose a much smaller parasitic mass on the truss than an equivalent active and passive approach.

FUTURE WORK

In the future, data with significantly less noise will be used to validate the physics model. Obtaining such data will require a more suitable test-bed. Also closed loop experimental data is needed to fully evaluate and confirm the suitability of MFC PZT patch actuators for the vibration suppression problem of solar sail booms. Finally, the issue of how to implement the shunting circuits in a space environment should be investigated.

ACKNOWLEDGMENTS

This research was funded by Grant Number NNM05AA13G from the National Aeronautics and Space Administration (NASA), Marshal Space Flight Center.

REFERENCES

1. D. Lichodziejewski, et. al. "**Bringing an Effective Solar Sail Design toward TRL 6**," *AIAA 2003-4659, Proc. 39th AIAA/ASME/SAE/ASEE Joint Propulsion Conference and Exhibit*, Huntsville, Alabama, (July 20-23, 2003).
2. D. Lichodziejewski, J. West, R. Reinert, K. Slade and K. Belvin, "**Development and Ground Testing of a Compactly Stowed Inflatably Deployed Solar Sail**," *AIAA Paper 2004-1507; Proc. 45th AIAA/ASME/ASCE/AHS/ASC Structures, Structural Dynamics and Materials Conference*, Palm Springs, California, (April 19-22, 2004).
3. D. W. Miller, E. F. Crawley, "**Theoretical and Experimental Investigation of Space-Realizable Inertial Actuation for Passive and Active Structural Control**," *AIAA Journal of Guidance, Control, and Dynamics*, Vol. 11, No. 5, pp. 449-458, (1988).
4. S. O. Moheimani, "**A Survey of Recent Innovations in Vibration Damping and Control Using Shunted Piezoelectric Transducers**," *IEEE Transactions on Control Systems Technology*, Vol. 11, No. 4, (July 2003).
5. J. Onoda, K. Makihara, and K. Minesugi, "**Energy-Recycling Semi-Active Method for Vibration Suppression with Piezo Transducers**," *AIAA Journal*, Vol. 41, No. 4, (April 2003).
6. O. Adetona, L.H. Keel, J.D. Oakley, K. Kappus, M.S. Whorton, Y.K. Kim, and J.M. Rakoczy, "**Model Correlation Study of a Retractable Boom for a Solar Sail Spacecraft**," 53rd *Joint Army-Navy-NASA-Air Force (JANNAF) Propulsion Meeting*, Monterey, CA, (December 5-9, 2005).
7. L. H. Keel, and O. Adetona, "**Model Correlation Study of a Retractable Boom for a Solar-sail Spacecraft**, " *Technical report submitted to Dr. Mark S. Whorton (NASA Technical Officer), EV42 / Guidance, Navigation, and Mission Analysis*, NASA Marshall Space Flight Center, AL, (September 14, 2005).
8. S. O. R Moheimani and A. J. Fleming, *Piezoelectric Transducers for vibration Control and Damping*, Springer, (June 2, 2006).
9. L. Meirovitch, *Analytical Methods in Vibrations*, Macmillan Publishing Co, Inc, New York, NY, 1967.
10. http://www.smart-material.com/media/Publications/MFCdata%2013-3-web.pdf
11. http://www.smart-material.com/MFC/P1_types.php